J Neurophysiol 124: 1615–1624, 2020.
First published September 30, 2020; doi:10.1152/jn.00285.2020.

RESEARCH ARTICLE | *Control of Movement*

Early stages of sensorimotor map acquisition: neurochemical signature in primary motor cortex and its relation to functional connectivity

F. T. van Vugt,[1,2,3] J. Near,[4,5] T. Hennessy,[4,5] J. Doyon,[3,6,7] and D. J. Ostry[1,2]

[1]*Department of Psychology, McGill University, Montreal, Quebec, Canada;* [2]*Haskins Laboratories, New Haven, Connecticut;* [3]*Department of Psychology, University of Montreal, Montreal, Quebec, Canada;* [4]*Douglas Mental Health University Institute, Montreal, Quebec, Canada;* [5]*Department of Biomechanical Engineering, McGill University, Montreal, Quebec, Canada;* [6]*Unité de Neuroimagerie Fonctionnelle, Centre de recherche, Institut universitaire de gériatrie de Montréal, Montreal, Quebec, Canada; and* [7]*Department Of Neurology and Neurosurgery, McGill University, Montreal, Quebec, Canada*

Submitted 27 May 2020; accepted in final form 23 September 2020

van Vugt FT, Near J, Hennessy T, Doyon J, Ostry DJ. Early stages of sensorimotor map acquisition: neurochemical signature in primary motor cortex and its relation to functional connectivity. *J Neurophysiol* 124: 1615–1624, 2020. First published September 30, 2020; doi:10.1152/jn.00285.2020.—The earliest stages of sensorimotor learning involve learning the correspondence between movements and sensory results—a sensorimotor map. The present exploratory study investigated the neurochemical underpinnings of map acquisition by monitoring 25 participants as they acquired a new association between movements and sounds. Functional magnetic resonance spectroscopy was used to measure neurochemical concentrations in the left primary motor cortex during learning. Resting-state functional magnetic resonance imaging data were also collected before and after training to assess learning-related changes in functional connectivity. There were monotonic increases in γ-aminobutyric acid (GABA) and decreases in glucose during training, which extended into the subsequent rest period and, importantly, in the case of GABA correlated with the amount of learning: participants who showed greater behavioral learning showed greater GABA increase. The GABA change was furthermore correlated with changes in functional connectivity between the primary motor cortex and a cluster of voxels in the right intraparietal sulcus: greater increases in GABA were associated with greater strengthening of connectivity. Transiently, there were increases in lactate and reductions in aspartate, which returned to baseline at the end of training, but only lactate showed a statistical trend to correlate with the amount of learning. In summary, during the earliest stages of sensorimotor learning, GABA levels are linked on a subject-level basis to both behavioral learning and a strengthening of functional connections that persists beyond the training period. The findings are consistent with the idea that GABA-mediated inhibition is linked to maintenance of newly learned information.

NEW & NOTEWORTHY Learning the mapping between movements and their sensory effects is a necessary step in the early stages of sensorimotor learning. There is evidence showing which brain areas are involved in early motor learning, but their role remains uncertain. Here, we show that GABA, a neurotransmitter linked to inhibitory processing, rises during and after learning and is involved in ongoing changes in resting-state networks.

Correspondence: D. Ostry (david.ostry@mcgill.ca).

GABA; learning; MRS; resting state; sensorimotor mapping

INTRODUCTION

When first learning a new motor skill, such as learning to speak or to play a musical instrument, the learner must establish which sensory outcomes (sounds in these examples) will result from which movements. During the earliest stages of learning, there is a paucity of prior information and the learner benefits little from existing strategies. How does one learn under these conditions? Behavioral studies have provided insight into the learning mechanisms (van Vugt and Ostry 2018a, 2019), but the brain implementation, in terms of the underlying functional reorganization and neurochemical changes, remains elusive. Here human participants learned a mapping between hand movements and sounds from scratch while we explored neurochemical changes in the primary motor cortex and obtained functional magnetic resonance imaging (fMRI) measures of resting-state functional connectivity to determine whether these changes were related to the amount of learning. The goal was to link changes in behavior that occur during the earliest stages of sensorimotor map acquisition to their underlying neurochemical mechanisms and to determine how brain functional connectivity measures reflect these neurochemical changes.

During the earliest stages of motor learning (Dayan and Cohen 2011; Krakauer et al. 2019), there is typically no prior control policy or sensorimotor map on which one can rely; therefore, learning proceeds de novo (Telgen et al. 2014). These earliest stages can be simulated in the laboratory by having participants make arm movements that are mapped to sounds (van Vugt and Ostry 2018a, 2019). Because arm movements are not normally linked to sounds, participants can be studied while they are in the unique situation of learning a novel mapping from scratch (van Vugt and Ostry 2018b) instead of adjusting an already learned mapping. A recent study showed that extensive practice in this task can yield an increasingly fine-grained performance (van Vugt and Ostry 2019). Yet, little is presently known about the brain areas involved in the early stages of this type of learning or the neurochemical processes that underlie their activity.

Previous work with magnetic resonance spectroscopy (MRS) has tracked concentrations of substances involved in neural signaling or metabolism and revealed changes in γ-aminobutyric acid (GABA) using a variety of learning paradigms. For example, during motor sequence learning, a reduction in GABA-mediated inhibition was observed in the primary motor cortex (Floyer-Lea et al. 2006; Kolasinski et al. 2019), which may allow the motor system to more rapidly execute movements. In contrast, measures of GABA based on intracortical inhibition showed that GABA-mediated inhibition is increased after learning (Cirillo et al. 2020), and data from perceptual and sensory association learning revealed an increase in GABA thought to enable stabilization of newly learned information (Shibata et al. 2017; Zheng and Knudsen 1999, 2001). Taken together, different learning mechanisms may cause learning-related increases or decreases in GABA. In addition to changes in GABA, previous work in the visual cortex has observed transient task-related increases in lactate and glutamate and decreases in aspartate and glucose (Bednarõík et al. 2015; Mangia et al. 2007) that are all presumably linked to oxidative metabolism, but it is uncertain whether these are associated with movement execution or instead are learning related. Lactate in particular has been linked to memory consolidation and modulation of neural excitability (Magistretti and Allaman 2018), which leads to the hypothesis that its involvement in motor learning may be learning related. In the functional domain, motor learning has been associated with changes in brain connectivity between a wide range of areas (Albert et al. 2009; Bernardi et al. 2018; Ma et al. 2011; Sami et al. 2014; Vahdat et al. 2011). It remains unclear whether and how these changes in functional connectivity are linked to neurochemical changes.

Here, we explored the neurochemical changes in the earliest stages of the acquisition of a novel audiomotor map and how these changes are linked to behavioral learning and associated changes in functional connectivity. Functional magnetic resonance spectroscopy (fMRS) was used before, during, and after training, to assess which chemical concentrations changed during training and whether the changes persisted during subsequent rest periods. The present study focused on the primary motor cortex since it has been found to be involved in a variety of motor learning tasks, especially in the earliest stages of learning (Hamel et al. 2017; Muellbacher et al. 2002; Orban de Xivry et al. 2011; Pascual-Leone et al. 1995; Rioult-Pedotti et al. 1998; Sanes and Donoghue 2000; but cf. Berlot et al. 2020; Kumar et al. 2019). We hypothesized that learning-related neurochemical concentration changes would correlate with the amount of learning observed behaviorally and with changes in functional connectivity patterns. Our main finding is that primary motor cortex GABA increases during and after training. The rate of this increase is correlated with the amount of behavioral learning and is linked to strengthening of functional connectivity between the left primary motor cortex (which is where GABA was measured) and the right intraparietal sulcus. This link between behavior, learning-related neurochemical change, and associated changes in brain connectivity identifies GABAergic processing as a key component of early sensorimotor map acquisition.

METHODS

Twenty-five healthy, right-handed participants (12 females, 13 males; mean age = 22.6 yr, SD = 3.5) were recruited for the study. Subjects had no formal musical training in the past 10 years and reported no neurological or hearing impairments. All subjects provided informed written consent, and the experimental protocol was approved by the McGill University, Faculty of Medicine Institutional Review Board (IRB).

Audiomotor learning task. Participants learned a new mapping between movements and sounds (van Vugt and Ostry 2018a, 2018b, 2019; for a similar paradigm, see Thompson et al. 2019) while they were in the MR scanner. On each trial, participants made a center-out reaching movement with their right hand using an MR-compatible joystick (Fig. 1, *A* and *B*). The movement angle was calculated online and was mapped systematically to a feedback sound consisting of three pure tones whose frequencies varied with the movement angle (Fig. 1*C*) and were presented over MR-compatible headphones. Before each trial, a target sound composed of the same three pure tones was presented. The target sound corresponded to an angle (in the mapping shown in Fig. 1*C*) that was chosen from a uniform distribution between 0° and 180°. The participants' task was to make a movement that they thought would result in the same sound as the target sound. At the end of the movement, the feedback sound corresponding to their actual movement was presented. Two training blocks of 96 trials were administered. Learning was assessed before and after training by having participants make movements to 10 target sounds (equally spaced across the workspace and presented twice in random order) without receiving feedback (no-feedback trials, see Fig. 1*D* for timing). Reaching error was assessed as the absolute angular distance between the angle corresponding to the target sound and the angle of the produced movement (in degrees). Note that sounds were not acoustically localized in space but rather were presented with equal intensity at each ear so that like speech sounds they differed only in their frequency content.

Procedure. In sequence, participants performed no-feedback trials and two baseline resting blocks, one during which fMRI and one during which fMRS baseline (pretraining) data were collected. Then two training blocks (train1, train2) were administered while collecting fMRS followed by resting (posttraining) fMRS and fMRI blocks (Fig. 1*D*). Subjects were asked to keep their eyes closed during fMRS scans (rest and task) but open during fMRI blocks. The 20 no-feedback trials before learning were divided into two blocks of 10 so that all the resting fMRI and fMRS blocks before and after training were immediately preceded by movements. Learning-related changes were assessed by correlation with behavioral measures of learning. Reaching error was averaged for the no-feedback trials before and after learning, and their difference is the estimate of learning that we then correlated with MRS measures. The neurochemical and functional connectivity analyses focused on identifying brain changes that were correlated with behavioral measures of learning. Nonspecific brain changes that are due to repetition of movements or the prolonged time in the scanner will presumably not correlate with the amount of learning. In this way, we tested for the specificity of the effects. We also tested for the specificity of the effects by assessing whether functional connectivity changes were likewise correlated with changes in neurochemical concentrations.

Behavioral data analysis and statistics. To analyze the behavioral data, reaching error was calculated as the absolute angular difference between the participant's movement direction and the direction associated with the target sound. For each participant, the errors were averaged within the pre and post no-feedback blocks and statistically compared using an ANOVA with the dependent variable being reaching error and the within-subject factor being time point (pre, post). The measure of behavioral learning imported into the MRS and fMRI analyses was the average absolute angular error during the post block divided by the pre block.

To test whether subjects came to the task with a prior map, we correlated the target angle with the movement angle for each of the no-feedback premovements, yielding one correlation value for each subject. These correlation values were then statistically compared against zero using a *t* test (reported as equivalent ANOVA). This was repeated for

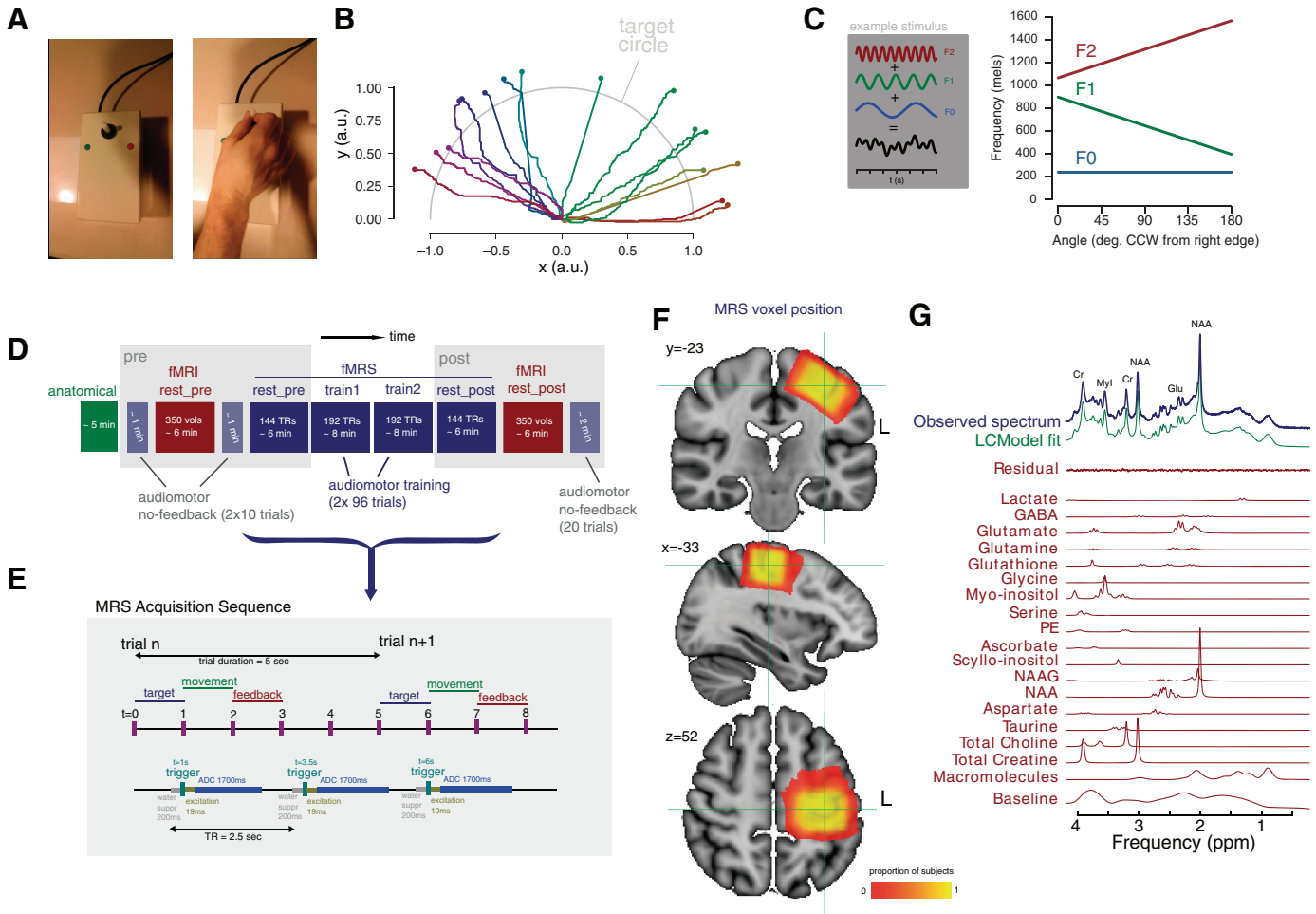

Fig. 1. Participants acquired a novel auditory-motor map while concentrations of neurochemical substances were scanned using magnetic resonance spectroscopy (MRS) and changes in functional brain networks were measured using resting-state functional magnetic resonance imaging (fMRI). *A*: participants used an MR-compatible joystick to move to auditory targets, and they received auditory feedback over headphones. *B*: example movements. The angle of the movement was mapped systematically to sounds. *C*: the target and feedback sounds consisted of combinations of three pure tones whose frequencies depended on the angle of the movement. *D*: design of the experiment; resting blocks were alternated with movement trials and MRS or fMRI was acquired. *E*: structure of a single trial (5 s) during which participants received a target sound, made a movement, and received feedback sound (1 s each) aligned with the MRS pulse sequence. *F*: the MRS data were acquired from a voxel placed based on each individual subject's anatomy and shown here warped to Montreal Neurological Institute (MNI) space. *G*: MRS data, after preprocessing, consisted of a spectrum (blue) that is essentially a linear combination of signatures of various metabolites (red), which were disentangled by a fitting procedure (green) that resulted in coefficients that corresponded to the concentration estimates of each of the metabolites. ADC, analog-to-digital converter; Cr, creatine; Glu, glutamate; L, left; Myl, myo-inositol; NAA, *N*-acetylaspartate; NAAG, *N*-acetylaspartylglutamate; PE, phosphatidylethanolamine; post, posttraining; pre, pretraining; TRs, repetition times; train1 and train2, training blocks 1 and 2.

the post no-feedback block. To test whether subjects' movements were more similar when these were to the same target, we computed the absolute angular distance between movements for pairs of targets during the pretraining block. If subjects based their movements on an existing sensorimotor map, we expected that a pair of movements to two presentations of the same target should be more similar (lower angular distance) than a pair of movements to two different targets. This procedure was repeated for the post no-feedback block.

Magnetic resonance spectroscopy. All imaging experiments were acquired on a Siemens (Erlangen, Germany) 3-Tesla Magnetom Trio MRI system with a body coil transmitter and a 32-channel head receiver array. First, a T1-weighted anatomical image was acquired using MPRAGE (Magnetization Prepared Rapid Gradient Echo; Mugler and Brookeman 1990; TR = 2,300 ms; TE = 2.98 ms; inversion time (TI) = 900 ms; flip angle = 9°; FOV = 256 mm; voxel size = 1 mm^3 isotropic; PAT = 2). The T1 image was used both for fMRI data analysis and for voxel placement during the MRS scans. An MRS voxel measuring 3 × 3 × 2 cm was centered over the hand knob of the left primary motor cortex (Yousry et al. 1997). To avoid inclusion of extracranial tissue, the voxel was rotated so that its large (3 × 3 cm) face was parallel with the surface of the brain (Fig. 1*F*). Across subjects, the pairwise overlap between MRS voxels as assessed by the Dice coefficient was 0.71 (SD = 0.10). The average percentage of white matter in the voxel was 48.9% (SD = 10.9%), gray matter was 36.1% (SD = 8.1%), and cerebrospinal fluid (CSF) was 14.8% (SD = 17.5%). The localized voxel was shimmed using the second-order shimming tool FAST(EST)MAP (Gruetter and Tkácõ 2000), and water was suppressed using the WET preparation module (Ogg et al. 1994). Localized MRS data were acquired using a Point RESolved Spectroscopy (PRESS) sequence (Bottomley 1987), optimized in-house (Fig. 1*E*) to achieve short echo times [TE = 19 ms; TR = 2,500 ms; vector size = 2,048; spectral width (SW) = 1,200 Hz]. Eight water reference PRESS averages were first acquired for coil combination and eddy current correction, followed by 144 water-suppressed averages during the pre block, 192 averages during each of the training blocks (train1 and train2), and another 144 averages during the post block. The resulting scan times were 6 min for the pre and post blocks and 8 min for the training blocks.

The PRESS sequence is not typically used to measure GABA. However, we hypothesized that detection of dynamic GABA changes against a relatively constant background signal should be feasible with this

sequence. It was previously shown that GABA levels are detected reproducibly in simulated short-TE MRS data, even when the unknown concentrations of all other metabolites and macromolecules were allowed to vary (Near et al. 2013). In that study, the simulated short-TE MRS data were similar in quality and appearance to the experimental data acquired in the current study. Furthermore, although MEGA-PRESS (MEshcher-GArwood Point RESolved Spectroscopy) is arguably better for detecting between-subjects differences in GABA, we argue that it is less optimal for detecting dynamic changes within individual subjects because *a*) it suffers from reduced signal efficiency compared with short-TE MRS (Near et al. 2011), and *b*) it is more sensitive to frequency drift and subject motion compared with short-TE MRS (Harris et al. 2014). To ensure that the MRS sequence used in the present study can reliably detect dynamic changes in GABA levels, we performed simulations in which we created a synthetic time series of spectra where we progressively varied the levels of GABA, glucose, lactate, and aspartate and confirmed that these changes could successfully be recovered using our analysis procedure (all Supplemental material is available at https://doi.org/10.6084/m9.figshare.12339257.v1).

Preprocessing of MRS data was performed in MATLAB using the FID-A tool kit (Simpson et al. 2017). First, the RF channels were combined for each block using the initial water reference scan to determine the optimal coil weightings. To remove any influence of scanner drift on subsequent metabolite quantification estimates, all four blocks (pre, train1, train2, and post) were then concatenated into a single time series, and spectral registration (Near et al. 2015) was used to correct frequency and phase drifts across all blocks simultaneously. Following spectral registration, an automated outlier removal procedure was applied to detect and remove individual averages that were corrupted by subject motion, and a frequency-referencing and phase-correction step was applied to the resulting time series. The data were then separated back into the pre, train1, train2, and post blocks, and each block of averages was combined. The residual water signal was then removed from each block using a Hankel–Lanczos singular-value decomposition (HLSVD) (Cabanes et al. 2001) water removal step. Finally, the linewidth of each final averaged block was corrected to account for blood-oxygen-level-dependent (BOLD)-induced changes in linewidth over time.

Processed spectra were fit in LCModel (Provencher 1993) using a simulated basis set that accounted for the specific timings and RF waveforms used in the optimized PRESS acquisition (Fig. 1*G*). The default LCModel baseline parameters and macromolecule setting were used. The average Cramer–Rao lower bound (CRLB) values were as follows: lactate = 12.8 (min = 7; max = 43), aspartate = 5.8 (min = 4; max = 15), glx (glutamate + glutamine) = 3.2 (min = 2; max = 6), GABA = 13.3 (min = 10; max = 22), and glucose = 17.3 (min = 6; max = 526). All metabolite concentrations were referenced to the sum of *N*-acetylaspartate (NAA) and *N*-acetylaspartylglutamic acid (NAAG; the key findings of the study, however, also held when referencing to total creatine instead). Outliers were removed using the boxplot rule, discarding datapoints that were further than 1.5 times the interquartile range away from the first or third quartile for a particular substance. To estimate glutamate, we used glx (glutamate + glutamine) as a surrogate because there is significant overlap between glutamate (glu) and glutamine (gln) at 3T, and therefore, it can be misleading to report only glutamate or glutamine levels alone (Hancu and Port 2011; Mullins et al. 2008; Öz et al. 2020). The average NAA linewidth was 6.98 Hz, range = 5.15–8.96 Hz. The average signal-to-noise ratio (as measured by the height of the NAA peak divided by the standard deviation of the noise between −2 ppm and 0 ppm) of the spectra was 289, range = 137–368. Finally, to rule out cross-contamination of metabolite measures, we evaluated the correlation between the LCModel concentration estimates for each pair of metabolites (see Supplemental material at https://doi.org/10.6084/m9.figshare.12339422.v1). The absolute values of the correlation coefficients ($|r|$) averaged across all subjects, and excluding self-correlation, were smaller than 0.5 for all pairs of metabolites of interest, including lactate (min = −0.05; max = 0.08), aspartate (min = −0.13; max = 0.10), glx (min = −0.25; max = 0.16), GABA (min = −0.09; max = 0.11), and glucose (min = −0.21; max = 0.32). We investigated the normality of the distribution of substance concentrations using the Shapiro−Wilk method. For none of the substances did Shapiro−Wilk indicate departure from normality (all $W > 0.93$, $P > 0.11$).

To assess changes from baseline, for each substance, the concentration (referenced to total NAA) was divided by the estimate for that substance during the pre block and expressed as a percentage change on a subject-level basis. Based on previous work, aspartate, glutamate, and lactate were expected to change transiently, and to estimate this, we computed their average concentration during the training blocks (train1 and train2) combined relative to baseline (pre). This was then statistically compared with baseline using a paired *t* test. Separately, the post-learning concentrations were compared against the pre values using a paired *t* test to confirm that concentrations had returned to baseline. GABA and glucose showed largely monotonic increases over the four blocks, and the rate of this change was estimated by fitting a regression line to the concentrations over the four blocks. To assess whether the increases were significant on the group level, the correlation coefficients for the subjects were submitted to an unpaired *t* test. Given the exploratory nature of the present study, uncorrected *P* values are reported. We then computed the correlation between the slope of this line (representing percentage change per block) with the amount of learning on the audiomotor task. To assess how GABA change was reflected in functional connectivity, we entered the GABA slope as a regressor in the resting-state fMRI analysis.

Resting-state functional magnetic resonance imaging. Functional images were obtained using the simultaneous multislice BOLD-EPI WIP sequence (Setsompop et al. 2012) as follows: 2 × 2 × 2 mm voxels, slice acceleration factor = ×6, TR = 1,050 ms, TE = 30 ms, 78 slices [no gap; flip angle (FA) = 45°]. In each scan (before and after learning), 350 volumes were acquired in a total scan time of just over 6 min. Offline processing of MRI data involved aligning the T1 image to the Montreal Neurological Institute (MNI) template using Advanced Normalization Tools (ANTs) (Tustison et al. 2014) and segmenting into cerebrospinal fluid (CSF), white matter, and gray matter using Freesurfer (Dale et al. 1999). For each functional run, the first five volumes were discarded. Images were simultaneously motion-corrected and slice-time-corrected using Nipy's SpaceTimeRealign algorithm (Roche 2011) and were corrected for susceptibility artifacts based on N4-bias-corrected opposite-phase encoding images (anterior-posterior, i.e., AP, and its opposite PA) using AFNI 3dQwarp (Cox 1996). Denoising was performed by bandpass filtering (0.08–0.09 Hz) and regressing out five white matter and CSF CompCor components (Behzadi et al. 2007) as well as motion regressors. Functional images were aligned to the subject anatomy using Freesurfer boundary-based registration and blurred at 6 mm full width at half maximum (FWHM).

We asked which areas of the brain changed their functional connectivity with the primary motor cortex in proportion to the amount of change of GABA (slope). We then separately tested whether the change in functional connectivity was also correlated with behavioral measures of learning. Functional connectivity was computed using a seed placed in the primary motor cortex hand area (spherical region of interest at MNI coordinates $x = -39$, $y = -23$, $z = 55$, radius = 3 mm). The seed region for connectivity analysis was restricted to the primary motor cortex hand area because MRS data were acquired from this location. For each subject and each scan (pre, post), we created a whole brain connectivity map by extracting the average functional signal time course in the seed region and then Pearson-correlating this with the time course of every voxel in the brain. The subsequent connectivity maps were submitted to group analysis using FSL FLAME (FMRIB's Local Analysis of Mixed Effects) with factor time point (before versus after) and the amount of GABA change as covariates of interest. Cluster forming threshold was set at $z = 2.4$ and cluster-level significance at $P = 0.05$ cluster-corrected.

RESULTS

Subjects learned a novel sensorimotor mapping from scratch in which movements were mapped to sounds composed of pure

tone combinations. Reaching error, assessed by the absolute angular difference between the participant's movement direction and the direction associated with the target sound, decreased over the course of training (Fig. 2*A*) and was lower during posttraining no-feedback trials than pretraining ones [$F(1,24) = 31.74$, $P < 0.001$, $\eta^2 = 0.41$]. Subjects learned the map from scratch because on a group level, before training, the subjects' reach angles did not correlate with the target angle ($F[1,22] = 0.65$, $P = 0.43$) but did so after training [$F(1,22) = 31.12$, $P < 0.001$, $\eta^2 = 0.59$] (Fig. 2*B*). However, it was still possible that before training, individual subjects had their own individual map between movements and sounds, which cancelled each other out on the group level. To test for this possibility, we computed the angular distance between pairs of movements to the same targets or to different targets and found that these were not different before learning [$F(1,24) = 0.22$, $P = 0.64$], indicating that subjects showed no consistency in their reaching pattern (Fig. 2*C*). After learning, however, movements to the same targets were more similar than movements to different targets [$F(1,24) = 31.94$, $P < 0.001$], indicating that subjects had become consistent in their movement pattern (Fig. 2*D*). Our subsequent neuroimaging and neurochemical analyses focused on identifying changes that were correlated with the amount of learning. We also assessed the specificity of the learning-related changes by testing whether the functional connectivity changes were themselves correlated with the neurochemical changes.

Neurochemical changes in primary motor cortex during training were quantified by comparing their concentration during and after the training blocks with the baseline prelearning block (Fig. 3*A*). Glucose and GABA showed monotonic downward and upward trends, respectively (Fig. 3*A*), and regression lines were fit to the concentration over time, whose slopes were significantly nonzero for glucose [$t(24) = 3.37$, $P = 0.003$] and GABA [$t(24) = 2.50$, $P = 0.02$] (Fig. 3*B*). Of these two, only the

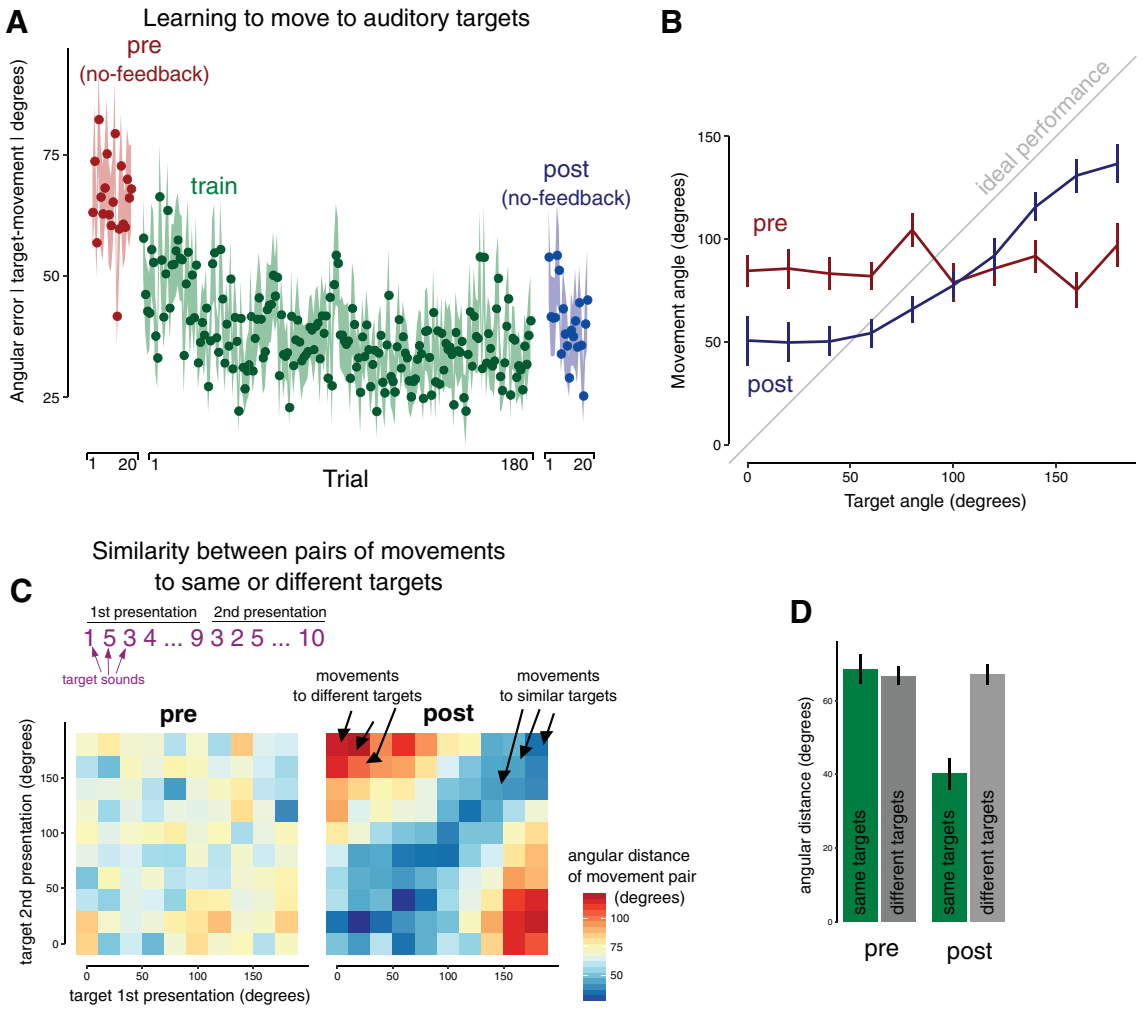

Fig. 2. Participants were involved in the earliest stages of learning in which little information was available initially and performance improved over the course of training. *A*: performance was estimated as the absolute angular error between the target location and subject's movement. This error decreased over time and maintained in postlearning no-feedback trials. *B*: initial reaching was not different across the different targets, but after learning, the angles of the movements reflected the target location. *C*: participants did not have a prior audiomotor map because there was no intraindividual consistency in reaching. Targets were presented twice in random order. Color scales indicate the distance between all possible pairs of movements to the first presentation (*horizontal*) and second presentation (*vertical*). Before learning (*left*), there was no difference between movements to similar targets (diagonal elements) or movements to different targets (off-diagonal elements) (see also *D*). After learning, movements to similar targets were more similar than movements to different targets, indicating the acquisition of a mapping that was not present before. post, Posttraining; pre, pretraining; train, training blocks.

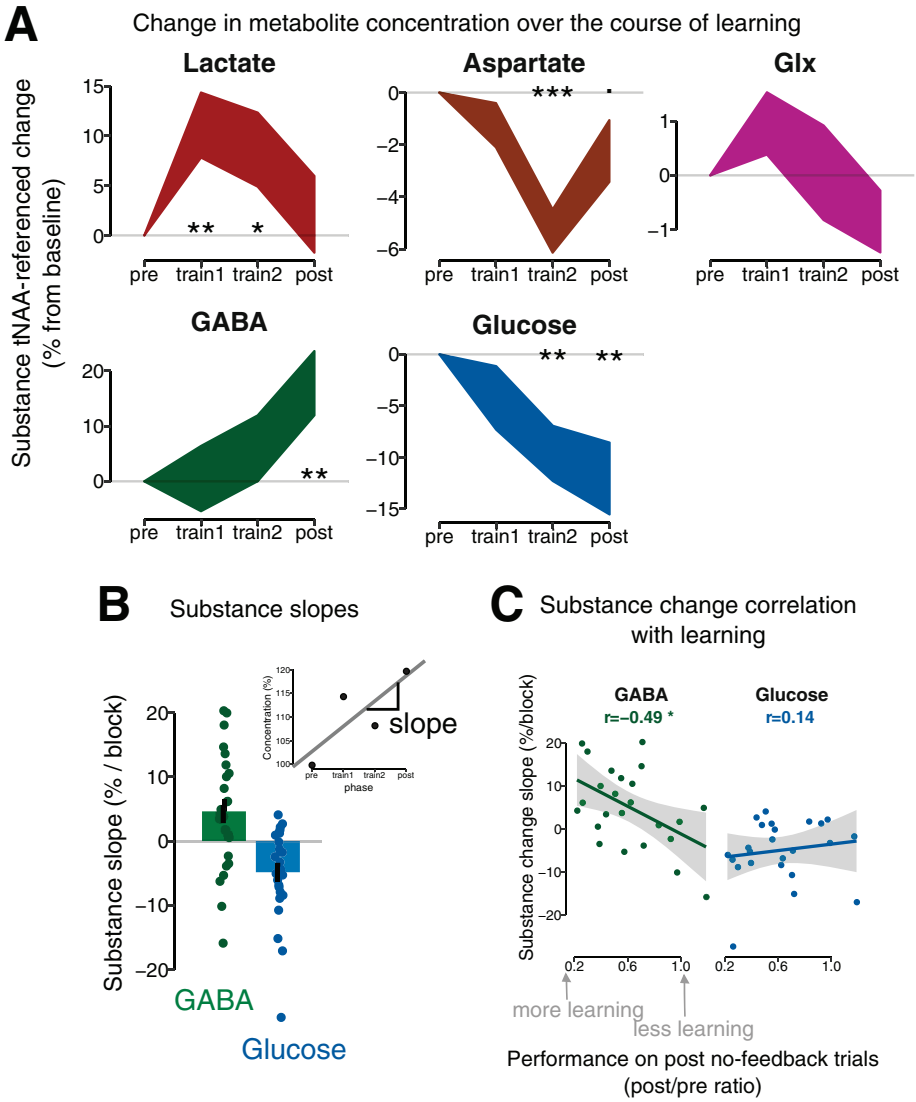

Fig. 3. GABA and glucose showed largely monotonic increases and decreases, respectively, that lasted beyond the end of training. The change in GABA concentration over the course of the experiment correlated with the amount of learning of the subjects. Transiently, lactate levels increased and aspartate decreased during learning but subsequently returned to baseline. *A*: vertical axes indicate the change in metabolite, referenced to total *N*-acetylaspartate (tNAA) concentration, as a percentage change from baseline levels. Blocks during which levels were significantly different from baseline are indicated: $*P < 0.05$, $**P < 0.01$; $***P < 0.001$. *B*: estimating the amount of change in each substance by fitting a regression line (*inlay*). Across subjects, the GABA slope was significantly positive and the glucose slope was significantly negative. *C*: correlating the estimated change of substances with the amount of learning reveals that only the change in GABA is learning-related. Glx, glutamate + glutamine; post, posttraining; pre, pretraining; train1 and train2, training blocks 1 and 2.

GABA change was correlated with the amount of behavioral learning of the subject (Pearson's $r = -0.49$, $P = 0.014$; other substances $P > 0.09$), where larger GABA slope increases were associated with greater learning (Fig. 3*C*). In addition, there were transient increases in lactate [$t(24) = 3.44$, $P = 0.002$] and reductions in aspartate [$t(24) = 4.06$, $P = 0.0005$] during training relative to (pre) baseline, which were no longer statistically significant postlearning (both $P > 0.07$; Fig. 3*A*). This transient change was not correlated with learning in the case of aspartate (Pearson's $r = 0.12$, $P = 0.59$) but in the case of lactate showed a trend toward statistical significance (Pearson's $r = 0.40$, $P = 0.05$). No significant changes in glx (glutamate + glutamine) were observed [$t(23) = 0.44$, $P = 0.67$].

The learning-related GABA change correlated with changes in resting-state functional connectivity between the left primary motor cortex (M1) and a cluster of voxels in the right intraparietal sulcus (IPS) (Fig. 4*A*). Before learning, functional connectivity between this cluster and the M1 seed region was not significantly different from zero [$t(24) = 1.04$, $P = 0.31$] but was positive after learning [$t(24) = 2.47$, $P = 0.02$] (Fig. 4*B*). The change in connectivity was confirmed to be correlated with the change in GABA (estimated as slope described above; Pearson's $r = 0.69$, $P = 0.0001$) where greater increases in GABA were associated with greater increases in functional connectivity (Fig. 4*C*). Furthermore, the change in connectivity was correlated with the amount of learning on a per-subject basis (Pearson's $r = -0.42$, $P = 0.04$; Fig. 4*C*), where subjects who learned more (lower error during the posttraining no-feedback trials) showed a greater increase in functional connectivity.

DISCUSSION

Subjects learned a novel mapping between movements and sounds (van Vugt and Ostry 2018a, 2018b, 2019), and we identified neural activity-related changes correlated with the amount of learning on a subject-level basis. This is a largely exploratory study that focuses on linking motor learning, resting-state connectivity, and the neurochemical substrates. Neurochemical measurements in the primary motor cortex showed monotonic increases in GABA during training, which extended into subsequent rest periods and were correlated

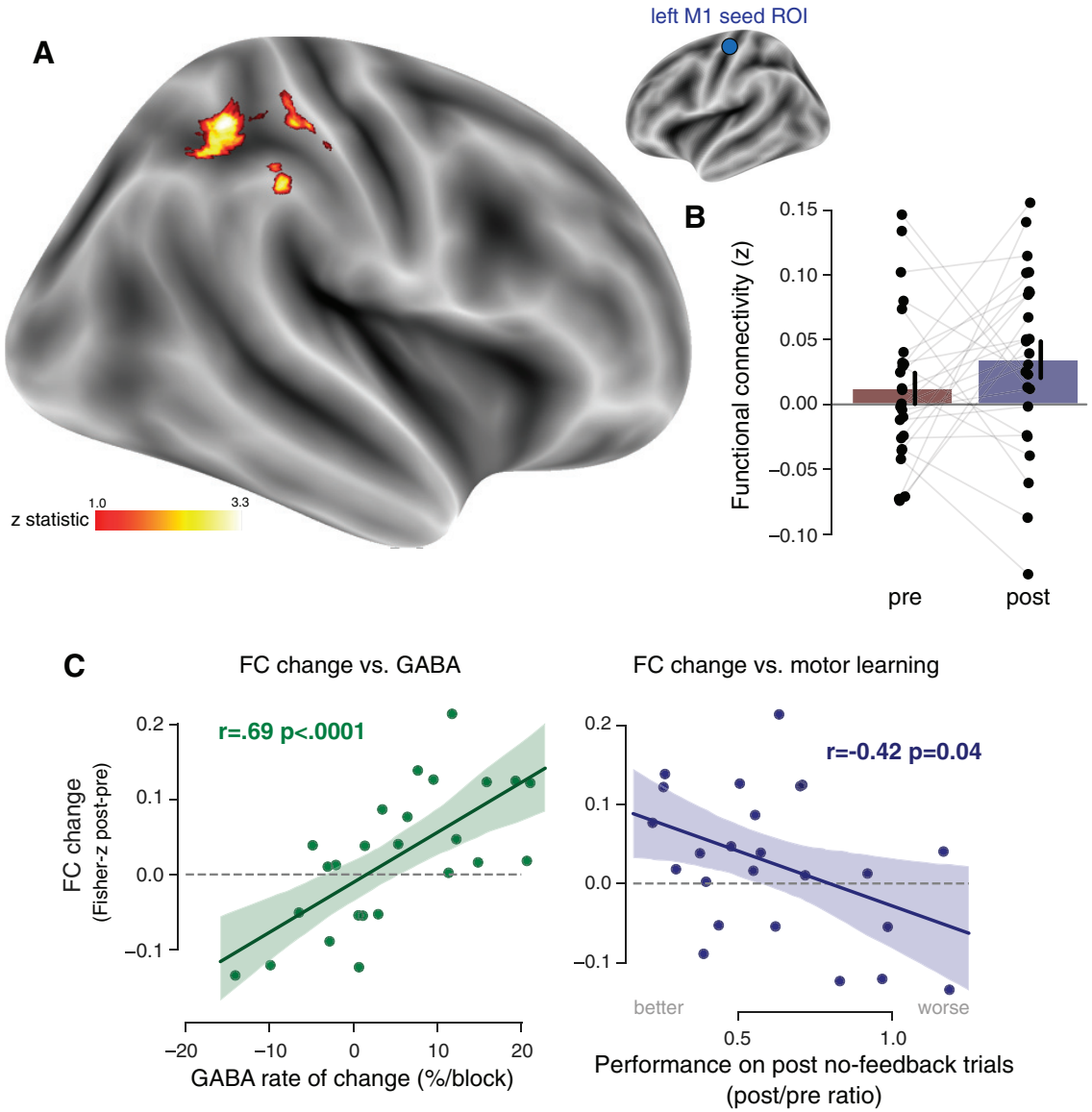

Fig. 4. Changes in GABA were correlated with the change in functional connectivity between the primary motor cortex and a set of voxels in the intraparietal sulcus (IPS). *A*: surface rendering of the voxels whose change in functional connectivity (FC) was correlated with the GABA change. *B*: functional connectivity (FC) was computed between the seed region and the cluster of voxels shown in *A*. Before training (pre), FC was not different from zero and was positive afterward (post) for those subjects who showed learning. Dots represent individual subjects, and error bars represent the standard error of the mean. *C*: graphical representation of the correlation, on an individual-subject level basis, between the change in functional connectivity (FC) from pre to post and the slope of GABA change. FC was found to be correlated with behavioral learning, where subjects who learned more showed greater increase in functional connectivity. M1, primary motor cortex; post, posttraining; pre, pretraining; ROI, region of interest.

with the amount of learning on a subject-level basis. The learning-related GABA increase also correlated with changes in resting-state functional connectivity observed after training. Specifically, greater increases in GABA were associated with greater increases in functional connectivity between the left primary motor cortex and a set of voxels in the right intraparietal sulcus (IPS). Transient increases in lactate and reductions in aspartate were also observed during training, as well as monotonic decreases in glucose that extended into the subsequent rest period, but only the lactate change showed a trend toward being correlated with learning. In summary, this study links GABA to both behavioral change and changes in functional connectivity during early learning of novel sensorimotor maps.

The primary motor cortex GABA concentration increased during training. In previous studies, both increases and decreases in GABA have been found in association with learning. Primary motor cortex GABA decreased during production of a motor sequence but only in a condition where learning was possible (Floyer-Lea et al. 2006; Kolasinski et al. 2019; Sampaio-Baptista et al. 2015). However, other work found that short-latency intracortical inhibition (SICI) increased following motor learning, which is thought to reflect an increase in GABA-mediated inhibition (Cirillo et al. 2020). In a similar vein, perceptual studies found increases in GABA in the primary visual cortex in conjunction with learning (Shibata et al. 2017). A further visual perceptual learning study showed that, depending on the task requirements, either increases or

decreases in GABA can occur (Frangou et al. 2019). Taken together with the present study GABA increase, it appears that the direction of GABA change depends on the nature of the learning task. During motor sequence learning, decreases in GABA-mediated inhibition may allow the motor system to execute movements more rapidly. Learning sensorimotor maps is part of an earlier stage of learning where the task is to create novel connections between sensory targets and motor responses. The capacity to maintain or stabilize newly learned information is thought to occur through predominantly GABA-mediated inhibitory processes (Shibata et al. 2017).

Individual differences in the rate of GABA change were correlated with learning; specifically, greater rates of GABA increase were associated with greater learning. To our knowledge, this is the first time that ongoing changes in GABA were found to be correlated with sensorimotor learning, which suggests that GABA plays a fundamental role in the acquisition process. Previous work has linked inhibitory processes to learning. For patients with visual neglect, it was shown that transcranial direct current stimulation (tDCS)-induced M1 disinhibition led to consolidation of prism adaptation learning (O'Shea et al. 2017). Motor sequence learning was found to be accompanied by changes in GABA, but these changes were not correlated with the amount of learning (Kolasinski et al. 2019). Instead, in that study, baseline GABA levels correlated with the amount of subsequent learning. Similarly, in another work, GABA-responsiveness to transcranial direct current stimulation (tDCS) was predictive of subsequent sequence learning (Stagg et al. 2011). In both of the aforementioned studies, less GABA was associated with more learning, which is opposite to that which was found here. A possible reason for this apparent incongruence is that in studies which have employed a sequence-learning paradigm, GABA's role may be to facilitate more rapid movement execution, whereas in the present work, learning did not involve movement speed but accuracy of sensory-to-motor responses. Correlational evidence in the same direction as shown here was reported in a cross-sectional study which found that higher GABA levels were associated with better performance on a battery of sensorimotor tasks (Cassady et al. 2019), but that study did not investigate learning. The finding of a correlation between the rate of GABA increase during training and the amount of learning is consistent with the idea that GABA-mediated inhibition may increase during learning so as to maintain newly learned information (Shibata et al. 2017). The idea that inhibition may serve to protect new memories is in line with opportunistic consolidation theory (Mednick et al. 2011), which proposes that consolidation of procedural hippocampus-dependent memories is initiated as soon as the brain is not occupied with encoding new memories, which can occur during certain sleep phases or as the result of substances such as *N*-methyl-D-aspartate receptor antagonists or alcohol. Although the present data focused on the primary motor cortex, it is possible that GABA increases played a similar role in reducing encoding of new memories to pave the way to consolidation of recently formed but still labile sensorimotor map memories.

Changes in GABA were reflected in functional brain connectivity measured at rest, where greater increases in GABA were associated with greater strengthening of connectivity between the primary motor cortex (where GABA was measured) and a set of voxels in the intraparietal sulcus (IPS). Motor learning was found to be accompanied by changes in functional connectivity at rest between a variety of areas including the primary motor cortex, premotor cortices, inferior and superior parietal cortex, cerebellum, putamen, and supplementary motor area (Albert et al. 2009; Bernardi et al. 2018; Sami et al. 2014; Vahdat et al. 2011). However, the neurochemical basis of these learning-related changes remains unclear. Previous neuroimaging work has used brain stimulation that results in altered GABA concentrations and, as in the present paper, found GABA-dependent changes in motor networks. Specifically, an anodal tDCS-induced decrease in M1 GABA correlated with an increase in fMRI-measured activity during the task (Stagg et al. 2011), similar to observations in the visual cortex (Bednarõík et al. 2015), as well as with an increase in motor network connectivity at rest (Stagg et al. 2014). A study in older adults also used tDCS to downregulate GABA and observed a reduction in interhemispheric resting-state functional connectivity and sensorimotor network strength (Antonenko et al. 2017). The present work is consistent with the latter finding showing that GABA increases resulting from a learning task are associated with increases in connectivity in functional motor networks. The intraparietal sulcus (IPS) identified here as a locus of functional change has previously been characterized as a sensory-motor interface for spatially coordinated movement (Grefkes et al. 2004) and as forming the intersection of areas coding concrete actions and their goals (Turella et al. 2020). The area is further implicated in the integration of visual and auditory reference frames, that is, a modality-unspecific coding of space (Mullette-Gillman et al. 2005), and in the manipulation of musical pitch information (Foster and Zatorre 2010). The present data, thus, link the IPS-M1 network to GABA increases and to behavioral improvements in learning novel sensorimotor maps.

The early stages of sensorimotor map learning were also found to be associated with a transient increase in aspartate and a decrease in lactate, both of which returned to baseline after training, as well as a decrease in glucose that lasted beyond training (cf. Shannon et al. 2016). These changes were not correlated with the amount of learning, except for lactate that showed a trend toward statistical significance. Although the present finding for lactate is not conclusive, its involvement in learning would be consistent with previous studies (Magistretti and Allaman 2018). Apart from the metabolic function of lactate, in which astrocytes produce lactate that is transported to neurons to meet neuronal energy demands (astrocyte-neuron lactate shuttle), lactate is also thought to be a signaling molecule involved in memory consolidation, as shown by data from the rat hippocampus during avoidance learning (Suzuki et al. 2011). Furthermore, several populations of neurons show increases in excitability in response to lactate (Magistretti and Allaman 2018). Thus, the present lactate finding may point to a learning-related role for lactate. The changes in aspartate, lactate, and glucose are also consistent with previous observations in the primary visual cortex in response to visual stimulation (Bednarõík et al. 2015; Mangia et al. 2007). Taken together with the present result that the changes in aspartate and glucose were not correlated with learning, it can be suggested that they reflect metabolic processes associated with the execution of movements and not learning. The decrease in glucose levels is likely due to an increase in the metabolic consumption of glucose (CMRglc) due to increased energy demands of performing the movement task. The reduced level of aspartate has been proposed to reflect an increased flux through the malate-aspartate shuttle, which is

used to replenish the cytosolic nicotinamide adenine dinucleotide (NAD)+ consumed by glycolysis (Mangia et al. 2007). Note that rather than recruiting a control group, we restricted our analyses to those changes that were correlated with the amount of learning, such as GABA. As a result, changes we observed that were not correlated with learning, such as aspartate and glucose, should be treated as tentative until future work validates these findings.

Unlike previous studies that also observed task-related glutamate increases in visual cortex (Bednarõík et al. 2015; Mangia et al. 2007), the present dataset did not reveal motor cortex glutamate changes. A possible reason for this is that the motor aspect of this task (moving a small joystick) was not sufficiently demanding to cause observable glutamate increases, and indeed, previous studies in the visual cortex showed the glutamate increase to be small in magnitude. Alternatively, previous studies did not investigate learning tasks, and thus, it is possible that learning involves an additional pathway for glutamate consumption that offsets any task-induced increase. Another possibility is that no glutamate change was observed because glutamatergic turnover can occur in milliseconds (Grewer et al. 2000), which makes it difficult to detect with the slow temporal resolution of the fMRS methods used here. However, it then remains unclear why previous studies (Shibata et al. 2017) did observe such a change.

In summary, the present study monitored participants as they form a novel mapping between movements and sounds to respond to auditory targets. We tracked neurochemical substances during learning and found that GABA increases monotonically during learning and beyond. The rate of this increase is correlated with learning and linked to strengthening of functional connectivity between the primary motor cortex (which is where GABA was measured) and the intraparietal sulcus. These observations situate GABA (or GABAergic processing) as an important mediator of behavioral change and functional brain connectivity that enable sensorimotor map acquisition.

GRANTS

This work was supported by National Institute of Child Health and Human Development R01 HD075740 and Fonds de recherche du Québec - Nature et technologies (FRQNT) (to D. J. Ostry); a Banting Fellowship BPF-NSERC-01098 and Canadian Institutes of Health Research (CIHR) Postdoctoral Fellowship #382252 (to F. T. van Vugt).

DISCLOSURES

No conflicts of interest, financial or otherwise, are declared by the authors.

AUTHOR CONTRIBUTIONS

F.T.V., J.N., T.H., J.D., and D.J.O. conceived and designed research; F.T.V., J.N., and T.H. performed experiments; F.T.V. and J.N. analyzed data; F.T.V., J.N., and D.J.O. interpreted results of experiments; F.T.V. prepared figures; F.T.V. drafted manuscript; F.T.V., J.N., T.H., J.D., and D.J.O. edited and revised manuscript; F.T.V., J.N., T.H., J.D., and D.J.O. approved final version of manuscript.

REFERENCES

Albert NB, **Robertson EM**, **Miall RC.** The resting human brain and motor learning. *Curr Biol* 19: 1023–1027, 2009. doi:10.1016/j.cub.2009.04.028.

Antonenko D, **Schubert F**, **Bohm F**, **Ittermann B**, **Aydin S**, **Hayek D**, **Grittner U**, **Flöel A.** tDCS-induced modulation of GABA levels and resting-state functional connectivity in older adults. *J Neurosci* 37: 4065–4073, 2017. doi:10.1523/JNEUROSCI.0079-17.2017.

Bednarõík P, **Tkácõ I**, **Giove F**, **DiNuzzo M**, **Deelchand DK**, **Emir UE**, **Eberly LE**, **Mangia S.** Neurochemical and BOLD responses during neuronal activation measured in the human visual cortex at 7 Tesla. *J Cereb Blood Flow Metab* 35: 601–610, 2015. doi:10.1038/jcbfm.2014.233.

Behzadi Y, **Restom K**, **Liau J**, **Liu TT.** A component based noise correction method (CompCor) for BOLD and perfusion based fMRI. *Neuroimage* 37: 90–101, 2007. doi:10.1016/j.neuroimage.2007.04.042.

Berlot E, **Popp NJ**, **Diedrichsen J.** A critical re-evaluation of fMRI signatures of motor sequence learning. *eLife* 9: e55241, 2020. doi:10.7554/eLife.55241.

Bernardi NF, **van Vugt FT**, **Valle-Mena RR**, **Vahdat S**, **Ostry DJ.** Error-related persistence of motor activity in resting-state networks. *J Cogn Neurosci* 30: 1883–1901, 2018. doi:10.1162/jocn_a_01323.

Bottomley PA. Spatial localization in NMR spectroscopy in vivo. *Ann N Y Acad Sci* 508: 333–348, 1987. doi:10.1111/j.1749-6632.1987.tb32915.x.

Cabanes E, **Confort-Gouny S**, **Le Fur Y**, **Simond G**, **Cozzone PJ.** Optimization of residual water signal removal by HLSVD on simulated short echo time proton MR spectra of the human brain. *J Magn Reson* 150: 116–125, 2001. doi:10.1006/jmre.2001.2318.

Cassady K, **Gagnon H**, **Lalwani P**, **Simmonite M**, **Foerster B**, **Park D**, **Peltier SJ**, **Petrou M**, **Taylor SF**, **Weissman DH**, **Seidler RD**, **Polk TA.** Sensorimotor network segregation declines with age and is linked to GABA and to sensorimotor performance. *Neuroimage* 186: 234–244, 2019. doi:10.1016/j.neuroimage.2018.11.008.

Cirillo J, **Semmler JG**, **Mooney RA**, **Byblow WD.** Primary motor cortex function and motor skill acquisition: insights from threshold-hunting TMS. *Exp Brain Res* 238: 1745–1757, 2020. doi:10.1007/s00221-020-05791-1.

Cox RW. AFNI: software for analysis and visualization of functional magnetic resonance neuroimages. *Comput Biomed Res* 29: 162–173, 1996. doi:10.1006/cbmr.1996.0014.

Dale AM, **Fischl B**, **Sereno MI.** Cortical surface-based analysis. I. Segmentation and surface reconstruction. *Neuroimage* 9: 179–194, 1999. doi:10.1006/nimg.1998.0395.

Dayan E, **Cohen LG.** Neuroplasticity subserving motor skill learning. *Neuron* 72: 443–454, 2011. doi:10.1016/j.neuron.2011.10.008.

Floyer-Lea A, **Wylezinska M**, **Kincses T**, **Matthews PM.** Rapid modulation of GABA concentration in human sensorimotor cortex during motor learning. *J Neurophysiol* 95: 1639–1644, 2006. doi:10.1152/jn.00346.2005.

Foster NEV, **Zatorre RJ.** A role for the intraparietal sulcus in transforming musical pitch information. *Cereb Cortex* 20: 1350–1359, 2010. doi:10.1093/cercor/bhp199.

Frangou P, **Emir UE**, **Karlaftis VM**, **Nettekoven C**, **Hinson EL**, **Larcombe S**, **Bridge H**, **Stagg CJ**, **Kourtzi Z.** Learning to optimize perceptual decisions through suppressive interactions in the human brain. *Nat Commun* 10: 474, 2019. doi:10.1038/s41467-019-08313-y.

Grefkes C, **Ritzl A**, **Zilles K**, **Fink GR.** Human medial intraparietal cortex subserves visuomotor coordinate transformation. *Neuroimage* 23: 1494–1506, 2004. doi:10.1016/j.neuroimage.2004.08.031.

Grewer C, **Watzke N**, **Wiessner M**, **Rauen T.** Glutamate translocation of the neuronal glutamate transporter EAAC1 occurs within milliseconds. *Proc Natl Acad Sci USA* 97: 9706–9711, 2000. doi:10.1073/pnas.160170397.

Gruetter R, **Tkácõ I.** Field mapping without reference scan using asymmetric echo-planar techniques. *Magn Reson Med* 43: 319–323, 2000. doi:10.1002/(SICI)1522-2594(200002)43:2<319:AID-MRM22>3.0.CO;2-1.

Hamel R, **Trempe M**, **Bernier P-M.** Disruption of M1 activity during performance plateau impairs consolidation of motor memories. *J Neurosci* 37: 9197–9206, 2017. doi:10.1523/JNEUROSCI.3916-16.2017.

Hancu I, **Port J.** The case of the missing glutamine. *NMR Biomed* 24: 529–535, 2011. doi:10.1002/nbm.1620.

Harris AD, **Glaubitz B**, **Near J**, **John Evans C**, **Puts NAJ**, **Schmidt-Wilcke T**, **Tegenthoff M**, **Barker PB**, **Edden RAE.** Impact of frequency drift on gamma-aminobutyric acid-edited MR spectroscopy. *Magn Reson Med* 72: 941–948, 2014. doi:10.1002/mrm.25009.

Kolasinski J, **Hinson EL**, **Divanbeighi Zand AP**, **Rizov A**, **Emir UE**, **Stagg CJ.** The dynamics of cortical GABA in human motor learning. *J Physiol* 597: 271–282, 2019. doi:10.1113/JP276626.

Krakauer JW, **Hadjiosif AM**, **Xu J**, **Wong AL**, **Haith AM.** Motor learning. *Compr Physiol* 9: 613–663, 2019 [Erratum in *Compr Physiol* 9: 1279, 2019]. doi:10.1002/cphy.c170043.

Kumar N, **Manning TF**, **Ostry DJ.** Somatosensory cortex participates in the consolidation of human motor memory. *PLoS Biol* 17: e3000469, 2019. doi:10.1371/journal.pbio.3000469.

Ma L, **Narayana S**, **Robin DA**, **Fox PT**, **Xiong J.** Changes occur in resting state network of motor system during 4 weeks of motor skill learning. *Neuroimage* 58: 226–233, 2011. doi:10.1016/j.neuroimage.2011.06.014.

Magistretti PJ, **Allaman I.** Lactate in the brain: from metabolic end-product to signalling molecule. *Nat Rev Neurosci* 19: 235–249, 2018. doi:10.1038/nrn.2018.19.

Mangia S, **Tkácō I**, **Gruetter R**, **Van de Moortele P-F**, **Maraviglia B**, **Uğurbil K.** Sustained neuronal activation raises oxidative metabolism to a new steady-state level: evidence from 1H NMR spectroscopy in the human visual cortex. *J Cereb Blood Flow Metab* 27: 1055–1063, 2007. doi:10.1038/sj.jcbfm.9600401.

Mednick SC, **Cai DJ**, **Shuman T**, **Anagnostaras S**, **Wixted JT.** An opportunistic theory of cellular and systems consolidation. *Trends Neurosci* 34: 504–514, 2011. doi:10.1016/j.tins.2011.06.003.

Muellbacher W, **Ziemann U**, **Wissel J**, **Dang N**, **Kofler M**, **Facchini S**, **Boroojerdi B**, **Poewe W**, **Hallett M.** Early consolidation in human primary motor cortex. *Nature* 415: 640–644, 2002. doi:10.1038/nature712.

Mugler JP III, **Brookeman JR.** Three-dimensional magnetization-prepared rapid gradient-echo imaging (3D MP RAGE). *Magn Reson Med* 15: 152–157, 1990. doi:10.1002/mrm.1910150117.

Mullette-Gillman OA, **Cohen YE**, **Groh JM.** Eye-centered, head-centered, and complex coding of visual and auditory targets in the intraparietal sulcus. *J Neurophysiol* 94: 2331–2352, 2005. doi:10.1152/jn.00021.2005.

Mullins PG, **Chen H**, **Xu J**, **Caprihan A**, **Gasparovic C.** Comparative reliability of proton spectroscopy techniques designed to improve detection of J-coupled metabolites. *Magn Reson Med* 60: 964–969, 2008. doi:10.1002/mrm.21696.

Near J, **Andersson J**, **Maron E**, **Mekle R**, **Gruetter R**, **Cowen P**, **Jezzard P.** Unedited in vivo detection and quantification of γ-aminobutyric acid in the occipital cortex using short-TE MRS at 3 T. *NMR Biomed* 26: 1353–1362, 2013. doi:10.1002/nbm.2960.

Near J, **Edden R**, **Evans CJ**, **Paquin R**, **Harris A**, **Jezzard P.** Frequency and phase drift correction of magnetic resonance spectroscopy data by spectral registration in the time domain. *Magn Reson Med* 73: 44–50, 2015. doi:10.1002/mrm.25094.

Near J, **Simpson R**, **Cowen P**, **Jezzard P.** Efficient γ-aminobutyric acid editing at 3T without macromolecule contamination: MEGA-SPECIAL. *NMR Biomed* 24: 1277–1285, 2011. doi:10.1002/nbm.1688.

O'Shea J, **Revol P**, **Cousijn H**, **Near J**, **Petitet P**, **Jacquin-Courtois S**, **Johansen-Berg H**, **Rode G**, **Rossetti Y.** Induced sensorimotor cortex plasticity remediates chronic treatment-resistant visual neglect. *eLife* 6: e26602, 2017. doi:10.7554/eLife.26602.

Ogg RJ, **Kingsley PB**, **Taylor JS.** WET, a T1- and B1-insensitive water-suppression method for in vivo localized 1H NMR spectroscopy. *J Magn Reson B* 104: 1–10, 1994. doi:10.1006/jmrb.1994.1048.

Orban de Xivry J-J, **Criscimagna-Hemminger SE**, **Shadmehr R.** Contributions of the motor cortex to adaptive control of reaching depend on the perturbation schedule. *Cereb Cortex* 21: 1475–1484, 2011. doi:10.1093/cercor/bhq192.

Öz G, **Deelchand DK**, **Wijnen JP**, **Mlynárik V**, **Xin L**, **Mekle R**, **Noeske R**, **Scheenen TWJ**, **Tkácō I**; **Experts' Working Group on Advanced Single Voxel 1H MRS.** Advanced single voxel ^{1}H magnetic resonance spectroscopy techniques in humans: experts' consensus recommendations. *NMR Biomed* e4236, 2020. doi:10.1002/nbm.4236.

Pascual-Leone A, **Nguyet D**, **Cohen LG**, **Brasil-Neto JP**, **Cammarota A**, **Hallett M.** Modulation of muscle responses evoked by transcranial magnetic stimulation during the acquisition of new fine motor skills. *J Neurophysiol* 74: 1037–1045, 1995. doi:10.1152/jn.1995.74.3.1037.

Provencher SW. Estimation of metabolite concentrations from localized in vivo proton NMR spectra. *Magn Reson Med* 30: 672–679, 1993. doi:10.1002/mrm.1910300604.

Rioult-Pedotti MS, **Friedman D**, **Hess G**, **Donoghue JP.** Strengthening of horizontal cortical connections following skill learning. *Nat Neurosci* 1: 230–234, 1998. doi:10.1038/678.

Roche A. A four-dimensional registration algorithm with application to joint correction of motion and slice timing in fMRI. *IEEE Trans Med Imaging* 30: 1546–1554, 2011. doi:10.1109/TMI.2011.2131152.

Sami S, **Robertson EM**, **Miall RC.** The time course of task-specific memory consolidation effects in resting state networks. *J Neurosci* 34: 3982–3992, 2014. doi:10.1523/JNEUROSCI.4341-13.2014.

Sampaio-Baptista C, **Filippini N**, **Stagg CJ**, **Near J**, **Scholz J**, **Johansen-Berg H.** Changes in functional connectivity and GABA levels with long-term motor learning. *Neuroimage* 106: 15–20, 2015 [Erratum in *Neuroimage* 116: 255, 2015]. doi:10.1016/j.neuroimage.2014.11.032.

Sanes JN, **Donoghue JP.** Plasticity and primary motor cortex. *Annu Rev Neurosci* 23: 393–415, 2000. doi:10.1146/annurev.neuro.23.1.393.

Setsompop K, **Gagoski BA**, **Polimeni JR**, **Witzel T**, **Wedeen VJ**, **Wald LL.** Blipped-controlled aliasing in parallel imaging for simultaneous multislice echo planar imaging with reduced g-factor penalty. *Magn Reson Med* 67: 1210–1224, 2012. doi:10.1002/mrm.23097.

Shannon BJ, **Vaishnavi SN**, **Vlassenko AG**, **Shimony JS**, **Rutlin J**, **Raichle ME.** Brain aerobic glycolysis and motor adaptation learning. *Proc Natl Acad Sci USA* 113: E3782–E3791, 2016. doi:10.1073/pnas.1604977113.

Shibata K, **Sasaki Y**, **Bang JW**, **Walsh EG**, **Machizawa MG**, **Tamaki M**, **Chang L-H**, **Watanabe T.** Overlearning hyperstabilizes a skill by rapidly making neurochemical processing inhibitory-dominant. *Nat Neurosci* 20: 470–475, 2017 [Erratum in *Nat Neurosci* 20: 1427, 2017]. doi:10.1038/nn.4490.

Simpson R, **Devenyi GA**, **Jezzard P**, **Hennessy TJ**, **Near J.** Advanced processing and simulation of MRS data using the FID appliance (FID-A)-An open source, MATLAB-based toolkit. *Magn Reson Med* 77: 23–33, 2017. doi:10.1002/mrm.26091.

Stagg CJ, **Bachtiar V**, **Amadi U**, **Gudberg CA**, **Ilie AS**, **Sampaio-Baptista C**, **O'Shea J**, **Woolrich M**, **Smith SM**, **Filippini N**, **Near J**, **Johansen-Berg H.** Local GABA concentration is related to network-level resting functional connectivity. *eLife* 3: e01465, 2014. doi:10.7554/eLife.01465.

Stagg CJ, **Bachtiar V**, **Johansen-Berg H.** The role of GABA in human motor learning. *Curr Biol* 21: 480–484, 2011. doi:10.1016/j.cub.2011.01.069.

Suzuki A, **Stern SA**, **Bozdagi O**, **Huntley GW**, **Walker RH**, **Magistretti PJ**, **Alberini CM.** Astrocyte-neuron lactate transport is required for long-term memory formation. *Cell* 144: 810–823, 2011. doi:10.1016/j.cell.2011.02.018.

Telgen S, **Parvin D**, **Diedrichsen J.** Mirror reversal and visual rotation are learned and consolidated via separate mechanisms: recalibrating or learning de novo? *J Neurosci* 34: 13768–13779, 2014. doi:10.1523/JNEUROSCI.5306-13.2014.

Thompson MMC, **Houde JF**, **Nagarajan SS.** Learning and adaptation in speech production without a vocal tract. *Sci Rep* 9: 13582, 2019. doi:10.1038/s41598-019-49074-4.

Turella L, **Rumiati R**, **Lingnau A.** Hierarchical action encoding within the human brain. *Cereb Cortex* 30: 2924–2938, 2020. doi:10.1093/cercor/bhz284.

Tustison NJ, **Cook PA**, **Klein A**, **Song G**, **Das SR**, **Duda JT**, **Kandel BM**, **van Strien N**, **Stone JR**, **Gee JC**, **Avants BB.** Large-scale evaluation of ANTs and FreeSurfer cortical thickness measurements. *Neuroimage* 99: 166–179, 2014. doi:10.1016/j.neuroimage.2014.05.044.

Vahdat S, **Darainy M**, **Milner TE**, **Ostry DJ.** Functionally specific changes in resting-state sensorimotor networks after motor learning. *J Neurosci* 31: 16907–16915, 2011. doi:10.1523/JNEUROSCI.2737-11.2011.

van Vugt FT, **Ostry DJ.** From known to unknown: moving to unvisited locations in a novel sensorimotor map. *Ann N Y Acad Sci* 1423: 368–377, 2018a. doi:10.1111/nyas.13608.

van Vugt FT, **Ostry DJ.** The structure and acquisition of sensorimotor maps. *J Cogn Neurosci* 30: 290–306, 2018b. doi:10.1162/jocn_a_01204.

van Vugt FT, **Ostry DJ.** Early stages of sensorimotor map acquisition: learning with free exploration, without active movement or global structure. *J Neurophysiol* 122: 1708–1720, 2019. doi:10.1152/jn.00429.2019.

Yousry TA, **Schmid UD**, **Alkadhi H**, **Schmidt D**, **Peraud A**, **Buettner A**, **Winkler P.** Localization of the motor hand area to a knob on the precentral gyrus. A new landmark. *Brain* 120: 141–157, 1997. doi:10.1093/brain/120.1.141.

Zheng W, **Knudsen EI.** Functional selection of adaptive auditory space map by GABAA-mediated inhibition. *Science* 284: 962–965, 1999. doi:10.1126/science.284.5416.962.

Zheng W, **Knudsen EI.** Gabaergic inhibition antagonizes adaptive adjustment of the owl's auditory space map during the initial phase of plasticity. *J Neurosci* 21: 4356–4365, 2001. doi:10.1523/JNEUROSCI.21-12-04356.2001.